Int. J. Heat Mass Transfer. Vol. 7, pp. 169–186. Pergamon Press 1964. Printed in Great Britain

MASS DIFFUSION IN NEUTRAL AND UNSTABLY STRATIFIED BOUNDARY-LAYER FLOWS

R. C. MALHOTRA* and J. E. CERMAK†

Fluid Dynamics and Diffusion Laboratory, College of Engineering, Colorado State University, Fort Collins, Colorado

(*Received* 5 *October* 1962 *and in revised form* 8 *July* 1963)

Abstract—Turbulent diffusion of matter from a point source within a two-dimensional boundary-layer flow over a smooth surface, with and without surface heating, has been studied. Concentrations downstream from a simulated point source located at the floor of a wind tunnel test section were measured using ammonia as the diffusing gas.

The concentration profiles for the neutral and unstable conditions are found to be similar; that is, a universal function is obtained by describing $\chi(x, y, z)/\chi_{max}(x, 0, 0)$ the relative concentration in each section as a function of the similarity lengths $\sigma(x)$ and $\eta(x)$. The similarity lengths are defined as $\chi(x, \sigma, 0)/\chi_{max}(x, 0, 0) = 0\,5$ and $\chi(x, 0, \eta)/\chi_{max}(x, 0, 0) = 0{\cdot}5$; they are found to be approximately independent of ambient velocity over the range of 6–25 ft/s and increase markedly in magnitude with increasing instability.

A method for numerically integrating point source data to obtain line source plumes is given. The synthetic line source plumes so obtained are compared with actual line source data and with line source heat diffusion data. The data for heat and mass diffusion are very similar.

An attempt is made to evaluate the ratio of heat and mass diffusivities by integrating the two-dimensional diffusion equation using the approximate similarity of the concentration and velocity distributions. An approximate value of 1·8 is found for this ratio.

NOMENCLATURE

A_z, vertical mass diffusivity, in z-direction, L^2/T;‡

a, b, n, exponents;

$C(x, z)$, mean concentration level of the diffusing matter—synthetic line source, M/L^3;

c_p, specific heat at constant pressure, Btu/Mt;

g, acceleration due to gravity, L/T^2;

$h(z/\lambda)$, $S_\lambda(z/\lambda)$, dimensionless functions;

p, standard deviation about the mean of the transverse profiles, L;

Q_f, Q_L, W/B, source strength for point source, synthetic line source and heat source respectively, M/T, M/LT, Btu/L^4T;

$\bar{t}(x, z)$, mean temperature at point (x, z) due to diffusion from a line source of heat, t;

$\bar{u}, \bar{w}$, components of mean velocity in the x and z-directions, L/T;

$\bar{U}_a$, mean ambient velocity in x-direction, L/T;

x, y, z, a right-hand co-ordinate system with origin at the source, L;

γ, molecular diffusion coefficient, L^2/T;

$\delta(x)$, boundary-layer thickness, L;

δ_t, thermal boundary-layer thickness, L;

ΔT, plate surface—ambient air temperature difference, t;

ϵ_H, coefficient of heat diffusion, L^2/T;

$\eta(x)$, vertical similarity length for the point-source diffusion plume, L;

* Assistant Professor. † Professor.

‡ The symbols designating dimensions have the following meaning: M—mass, L—length, T—time, t—temperature, Btu—heat unit.

$\lambda(x)$, vertical similarity length for the synthetic line source diffusion plume, L;
ν, kinematic viscosity, L^2/T;
ρ, mass density, M/L^3;
$\sigma(x)$, lateral similarity length for the point source diffusion plume, L;
$\chi(x, y, z)$, mean concentration level at the point (x, y, z) for diffusion from a ground-level point source, M/L^3.

INTRODUCTION

BOUNDARY-LAYER flows over horizontal heated surfaces are a common occurrence in industry and constitute the basic flow of the atmospheric surface layer much of the time. Heating of the boundary from below produces an instability through action of buoyancy forces which modifies the much studied neutral boundary-layer flow. This modification by interaction has been found to affect the drag and heat-transfer coefficients in a substantial manner. In an analysis of the laminar boundary layer over a heated plate, Sparrow and Minkowycz [1] have found an increase of the drag and heat-transfer coefficients to occur. An experimental study of turbulent boundary layers at low Reynolds numbers over a heated plate by Cermak [2] yielded an increasing drag coefficient for increasing degrees of instability. Associated with the modification of turbulent flow structure produced by thermal instability is an increase in diffusion rates for passive material released from sources located within the flow. This phenomenon is known to exist almost by instinct, from casual observation of smoke and other pollutants diffusing in the atmosphere and from detailed laboratory-type measurements of diffusion in the field made during Project Prairie Grass (Barad [3], Haugen [4]).

The purpose of the study reported in this paper was to compare diffusion rates and concentration-field geometry for a ground-level point source of ammonia gas in neutral and unstable turbulent boundary layers by making use of controlled wind tunnel flow. This information is itself useful to the heat transfer and air pollution engineer in solving certain practical problems, but perhaps even more important, is the knowledge it yields about the gross change in flow structure which provides a sound basis for study of the detailed structural changes. The data obtained for mass diffusion in a neutral boundary layer are also used in a comparison with heat diffusion data reported by Wieghardt [5] in an effort to establish the ratio of turbulent diffusivities for heat and for mass.

EQUIPMENT AND PROCEDURE

The diffusion study was conducted in a recirculating wind tunnel with a 6-ft square, 12-ft long test section. A schematic diagram of the test section is shown in Fig. 1. The components of the test section in Fig. 1 are labelled as follows:

A—turbulence stimulator,
B—aerodynamically smooth, heated or neutral test boundary, over which the momentum and the thermal boundary-layers developed,
C—the heating coils and thermal insulation,
D—sampling probe with tubing leading to sampling system,
E—point source of ammonia gas.

The turbulence stimulator consisted of a $\frac{3}{8}$-in saw-tooth strip followed by 24 in of closely packed gravel. This stimulator was followed by a smooth strip of wood and the test boundary.

The smooth, heated or neutral boundary was a 6×10 ft, $\frac{1}{2}$-in thick aluminium plate mounted flush with the floor of the wind tunnel. The plate was heated by groups of nichrome heating coils mounted directly below the plate; each group was connected to a rheostat by means of which the power input to each group could be adjusted to the desired value to give a uniform surface temperature for different flow conditions. The entire unit was connected through a variable voltage powerstat. Thus, using this equipment, it was possible to heat the plate to temperatures of more than 200°F above that of the ambient air for air speeds of up to 9 ft/s.

Before the start of experiments with a particular flow condition, the uniform temperature on

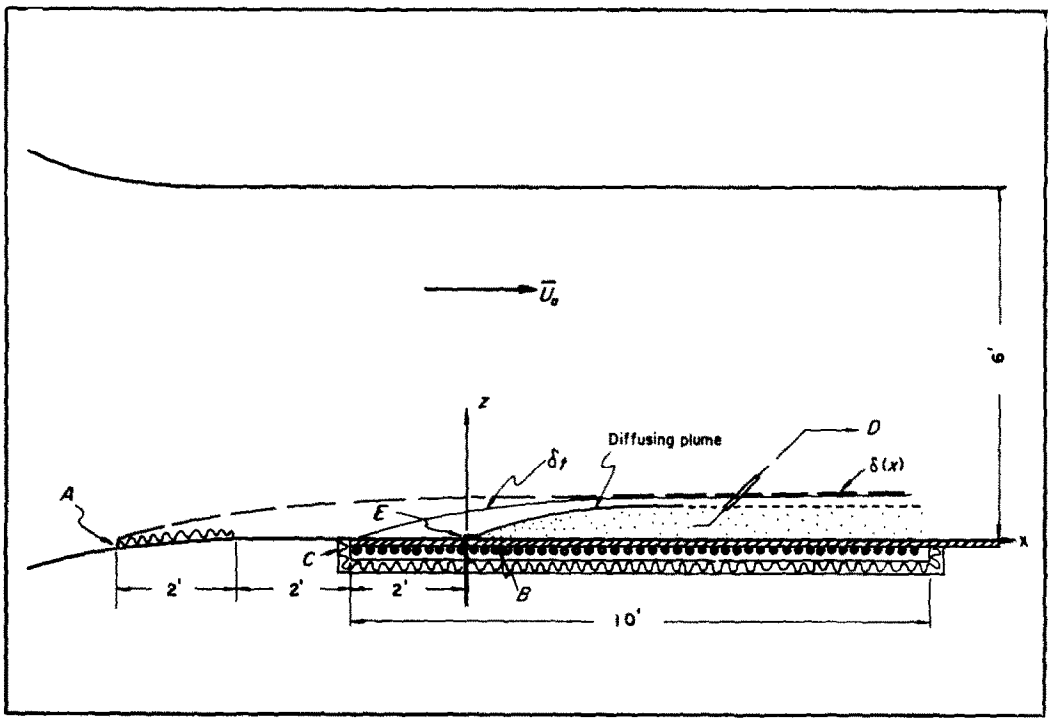

FIG. 1. Test section geometry.

the plate surface was obtained by adjusting the power input to the individual heater strips by trial and error. Once the rheostat settings were established for a particular flow condition, almost the same settings were used on subsequent days with the temperature distribution being checked each day.

The gas feed and sampling system used is schematically shown in Fig. 2. Anhydrous ammonia gas having a specific gravity of 0·6 relative to air were used as the diffusing gas. The gas was fed into the tunnel at a constant rate through a stainless steel feed probe. The mixture of the diffusing gas and air was drawn through the sampling system by inducing negative pressures with a vacuum pump. The sampling rate and the feed rate was measured by Matheson Universal Flowmeters.

The metered sample of air containing ammonia was passed through an absorption tube containing 10 cc of dilute hydrochloric acid, which completely absorbed the ammonia from the sample. The mixture in the absorption tube was subsequently neutralized by adding 1·2 cc of a dilute solution of sodium hydroxide. The neutralized sample containing the ammonia in solution was then mixed with 1 cc of Nessler's reagent, which gave a yellowish-brown coloration dependent on the concentration of ammonia present in the sample. The absolute quantity of ammonia was ascertained using an Evelyn Photo-electric Colorimeter which was previously calibrated by using a standardized solution containing 0·1 mg of ammonia in 1 cc of the solution.

Once the flow conditions were established vertical cross sections of the plume were mapped at $x = 1$, 2, 3, 4, 6, and $7\frac{1}{2}$ ft from the source. The following procedure was used in mapping the plume cross section, see Fig. 3:

(1) Lateral profiles of concentration measurement were made by traversing the sampling probe parallel to the y-axis for a fixed height z in. Sampling points were spaced between 0·25 to 1 in apart; about twenty

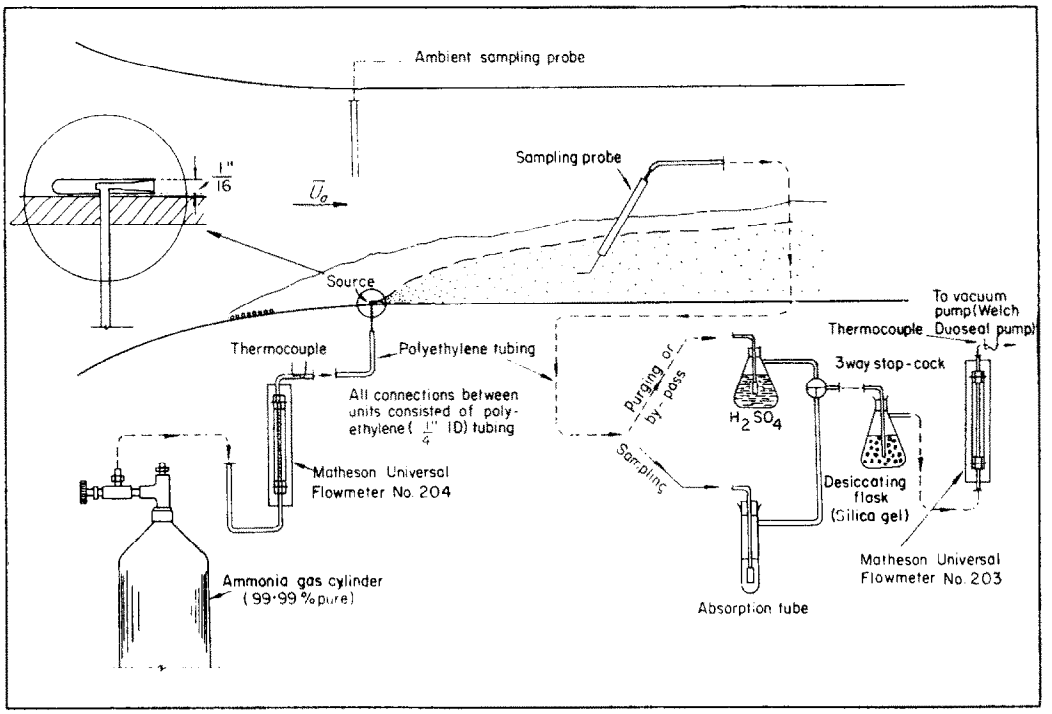

FIG. 2. Feed and sampling system.

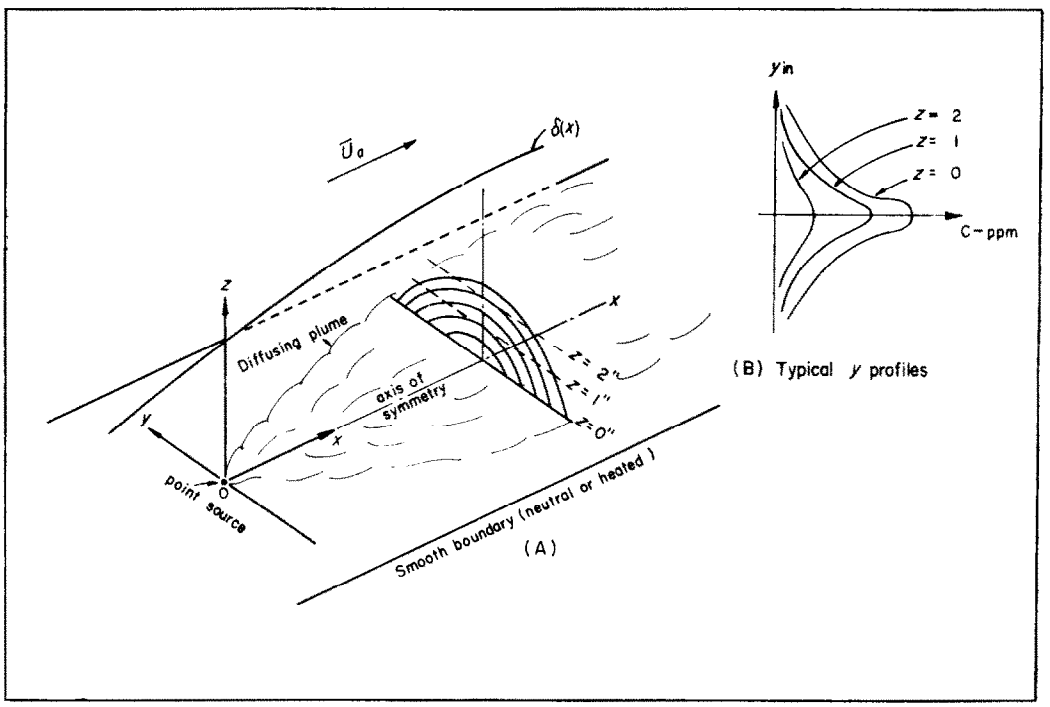

FIG. 3. Definition sketch of plume geometry.

point measurements were made per lateral profile.

(2) The lateral profiles were repeated for several heights $z = 0, 1, 2, \ldots$ in.

(3) The measured lateral profiles were superposed as in Fig. 3 (B).

(4) Isoconcentration contours were mapped by reading y-co-ordinates of points of equal concentration in Fig. 3 (B), and transposing to the plume cross section.

Besides the mean concentration data, the mean velocity and mean temperature fields were mapped for several cross sections downstream of the gas source; also, the heat input into the boundary was measured for the heated boundary runs. The mean velocity distributions were measured using a constant-temperature hot-wire anemometer. The mean temperature distributions were measured by means of a copper–constantan thermocouple. Both the hot-wire and the thermocouple probes were mounted on a carriage with remotely controlled three-dimensional motion. The upward flux of heat from the boundary was estimated by measuring the power input to each individual group of nichrome heating coils with an ammeter and voltmeter. Since the heat loss from the heating coils to the surroundings is negligible, the power input per unit area to the plate was the upward flux of heat from the heated boundary.

The data gathered was for the following combination of mean velocity $\bar{U}_a$ in ft/s and plate surface-ambient air temperature difference ΔT in degF: (6; 0), (9; 0), (6·5; 80), (6·5; 200) and (9; 115). In addition to the above data the boundary concentration downstream of the source was measured for (15; 0), (25; 0) and (57; 0). The experimental data is quite voluminous and thus readers are referred to Malhotra [6] for the details of the experimental apparatus and a summary of all the data gathered during the course of this study.

Discussion of accuracy of data

There are two gross checks on the accuracy of

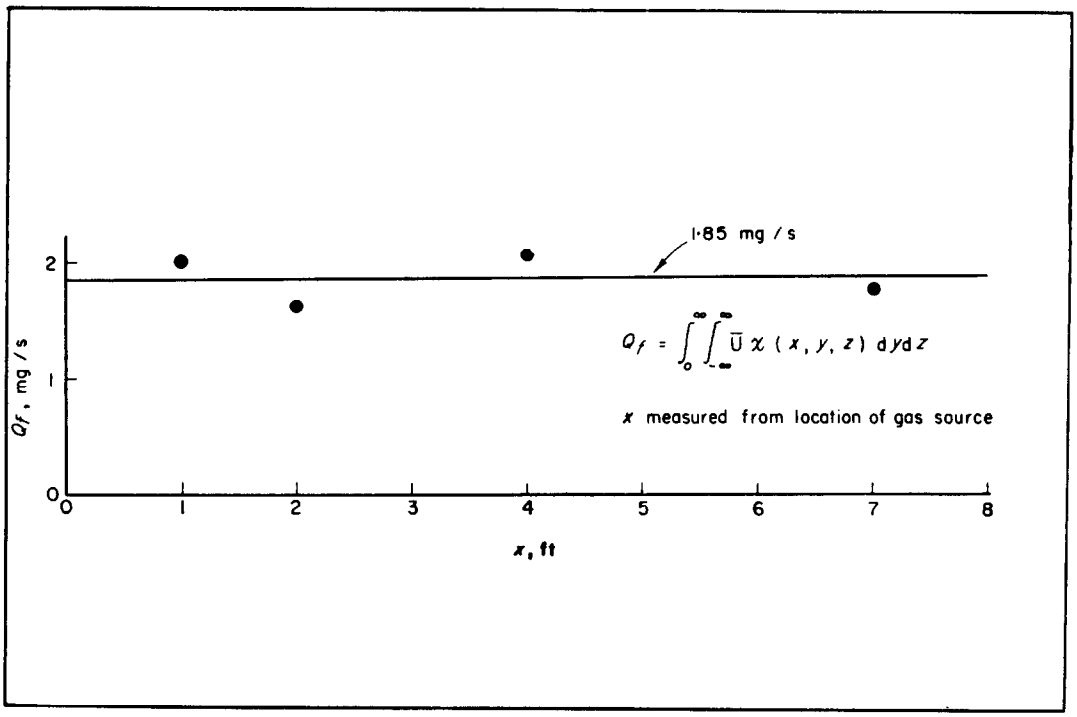

FIG. 4. Relative ground-level concentration as a function of the lateral distance for a point source with an unheated boundary.

the experimental data. One is to check the continuity of mass from cross section to cross section downwind of the gas source, i.e.

$$\int_{y=-\infty}^{\infty}\int_{z=0}^{\infty} \bar{u}\,\chi\,(x, y, z)\,\mathrm{d}z\,\mathrm{d}y \text{ all } x = Q_f = \text{const.}$$

The other is to duplicate the experimental data two or more times for any given cross section. Both these checks were made and it was estimated that the data could be duplicated to within 10 per cent at a concentration of 100 parts per million by weight (the data ranged between 50 ppm and 7000 ppm). Fig. 4 is a typical plot of the variation of Q_f with distance downstream of the source. As seen from this figure the mass of the diffusing gas is quite consistent as one moves downstream of the source.

EXPERIMENTAL RESULTS

Neutral boundary layer

The diffusion plume for the short distances studied, was completely submerged in the boundary layer. The concentration distribution can be described by a dimensionless universal curve, Figs. 5–7

$$\frac{\chi(x, y, z)}{\chi_{\max}(x, 0, 0)} = \exp 0{\cdot}693\left\{-\left[\frac{y}{\sigma(x)}\right]^a - \left[\frac{z}{\eta(x)}\right]^b\right\}, \quad (1)$$

where $\sigma(x)$ and $\eta(x)$ are the lateral and vertical similarity lengths of the diffusing plume defined as

$$\frac{\chi(x, \sigma, z)}{\chi_{\max}(x, 0, 0)} = 0{\cdot}5, \quad \frac{\chi(x, 0, \eta)}{\chi_{\max}(x, 0, 0)} = 0{\cdot}5,$$

with a and b being constants ($a = 2{\cdot}0$, $b = 1{\cdot}4$).

It can be noted from (1) that within the range of experimental variables the dimensionless concentration distribution function is independent of $\bar{U}_a$. Within this same range of variables Fig. 8 shows that the vertical and lateral growth of the plume, as characterized by the similarity

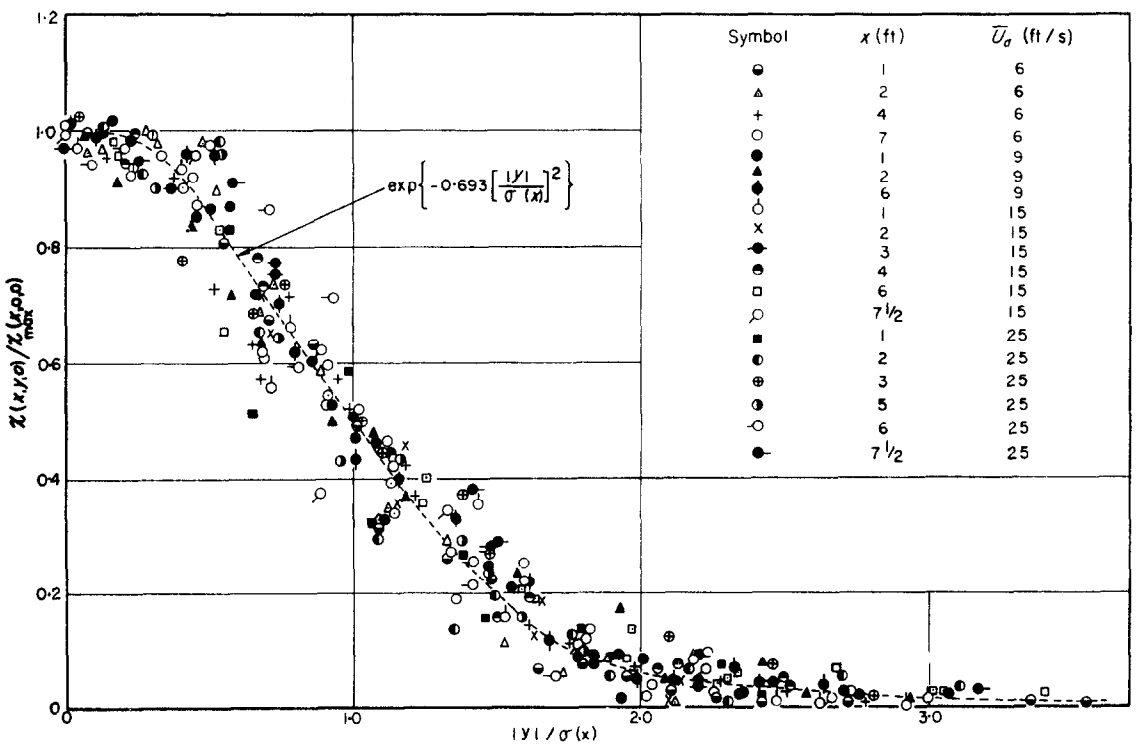

FIG. 5. Typical plot of integration of continuity equation for point source at various distances downstream of source.

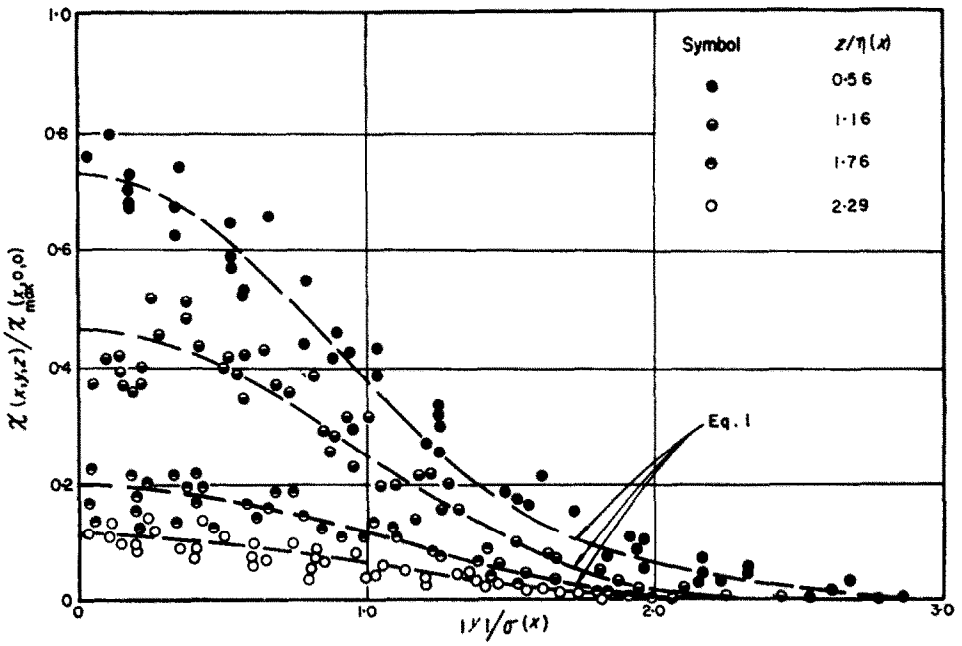

FIG. 6. Relative concentration as a function of the lateral distance for various elevations for a point source with an unheated boundary.

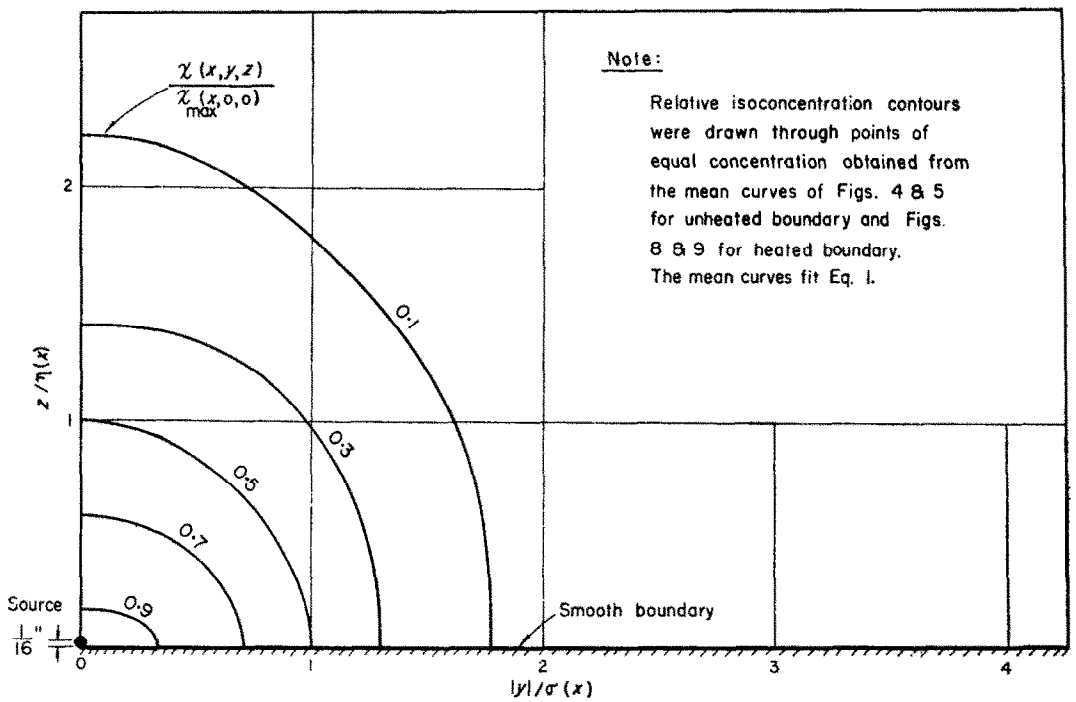

FIG. 7. Non-dimensional plume cross section for a point source with heated and unheated boundary.

lengths $\eta(x)$ and $\sigma(x)$ are also independent of $\bar{U}_a$ (6–25 ft/s). Their approximate proportionality with x is

$$\eta(x) = \text{const. } x^{0.71}, \tag{2a}$$

and

$$\sigma(x) = \text{const. } x^{0.60}. \tag{2b}$$

The corresponding values of $\chi_{\max}(x, 0, 0)$ appears to be inversely proportional to $\bar{U}_a$ as is shown in Fig. 8. The initial variation of $\bar{U}_a$ $\chi_{\max}(x, 0, 0)$ can be approximated by

$$\bar{U}_a \, \chi_{\max}(x, 0, 0) = \text{const. } x^{-1.5}. \tag{3}$$

The consistency of the experimental results may be checked by using (1) and (2) and the appropriate similarity equation of the mean velocity field:

$$\frac{\bar{u}}{\bar{U}_a} = \left(\frac{z}{\delta}\right)^{1/n}; \quad 0 \leqslant z < \delta \tag{4}$$

where, as determined from the measured mean velocity profiles, $n = 5{\cdot}5$ and $\delta \propto x^{0.23}$. These equations may be introduced into the integral form of the mass-conservation equation

$$\int_{y=-\infty}^{\infty} \int_{z=0}^{\infty} \bar{u} \chi \, dy \, dz = Q_f \tag{5}$$

to obtain an expression for $\bar{U}_a \chi_{\max}(x, 0, 0)$.

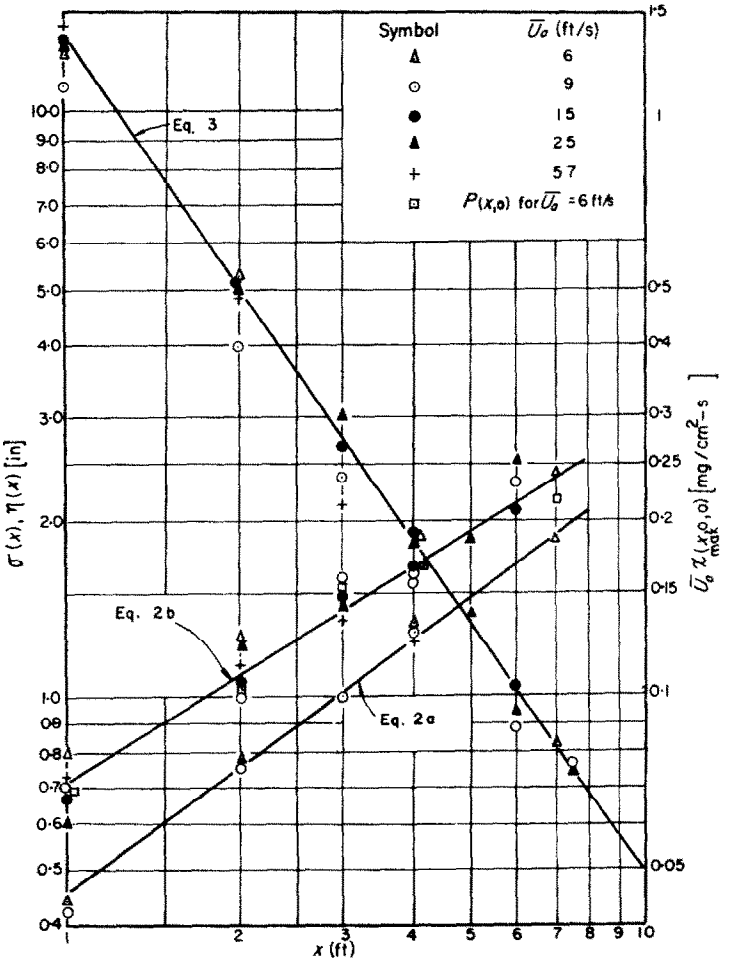

FIG. 8. Variation of the vertical and lateral similarity lengths σ and η and the maximum ground-level concentration with distance from the point source for an unheated boundary.

Noting that $z/\delta = z/\eta\,(\eta/\delta)$, it follows from (1), (4) and (5) that

$$\bar{U}_a\,\chi_{\max}(x,0,0) = \frac{a\,b\,Q_f\,(0{\cdot}693)^{2+1/nb}}{2\,\Gamma(1/a)\,[\Gamma(1+n/nb)]}\left(\frac{\eta}{\delta}\right)^{-1/n}(\eta\sigma)^{-1}.$$

Substituting the approximate proportionality of $\eta(x)$, $\sigma(x)$ and $\delta(x)$ with x into the above equation one finds that

$$\bar{U}_a\,\chi_{\max}(x,0,0) \propto x^{-1{\cdot}4}. \qquad (6)$$

A comparison of (3) and (6) shows the consistency of the experimental results for the neutral boundary.

Further, it should be kept in mind that the similarity lengths, $\sigma(x)$ and $\eta(x)$ cannot indefinitely grow at the same rate, i.e. linearly with distance; the plume growth must slow down when the mass reaches the upper edge of the boundary layer. Figs. V-27 to V-32 of Davar [7] actually show this trend for an elevated point source. A similar trend was observed by Poreh [8] for a ground-level line source where concentrations were measured up to 25 ft downstream from the source. Thus it seems that diffusion in wind tunnels is characterized by regimes or zones of spread; the zone reported on in this experimental study is one in which the mass plume is everywhere thinner than the momentum boundary-layer and is equivalent to conditions encountered in the lower atmosphere.

Unstable boundary layers

The concentration distribution for the heated-boundary experiments can be represented by the same distribution function as that for the neutral boundary (Figs. 7, 9 and 10), as given by (1), where σ, η and $\chi_{\max}$ are a function not only of the distance from the source, as was the case for the neutral boundary plume, but also of the instability produced by heating.

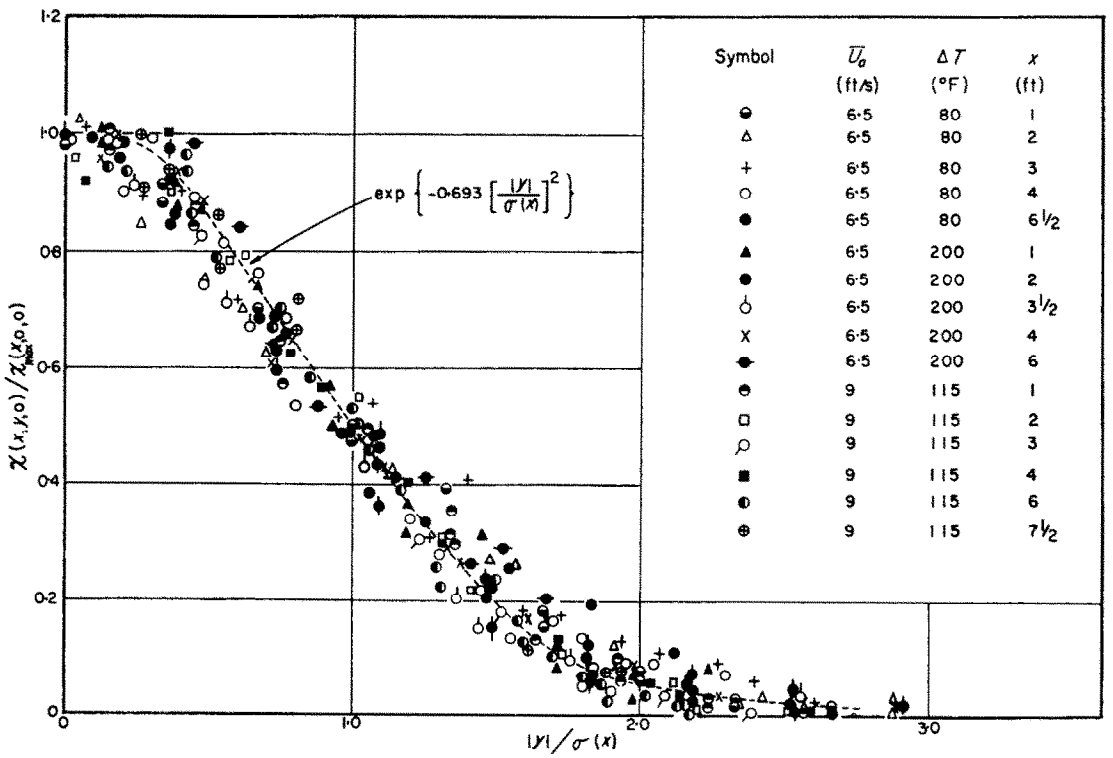

FIG. 9. Relative ground-level concentration as a function of the lateral distance for a point source with a heated boundary.

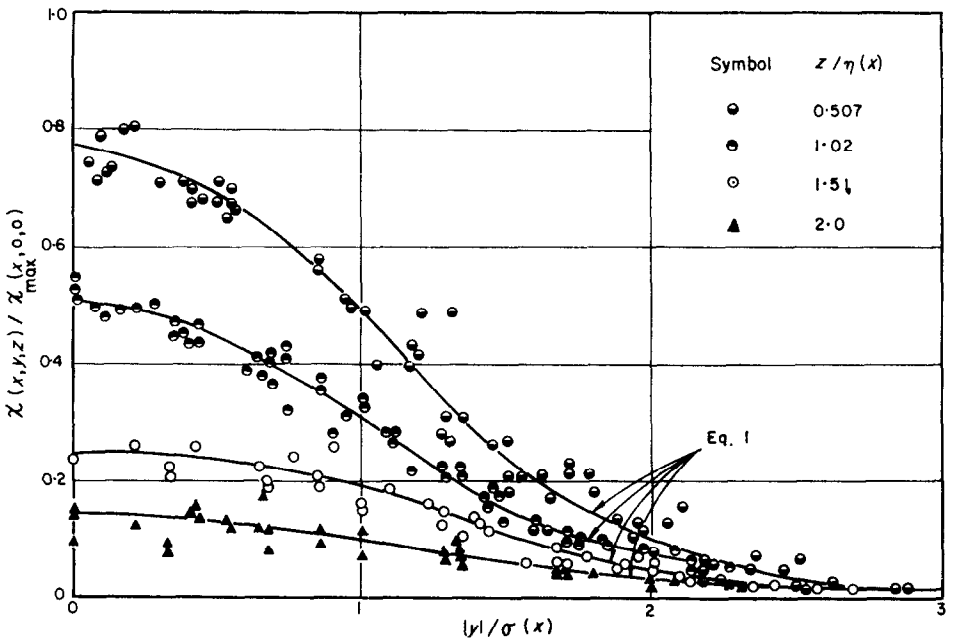

FIG. 10. Relative concentration as a function of the lateral distance for various elevations for a point source with a heated boundary.

Within the range of experimental variables studied the variation of χ_{max}, σ and η with distance follow simple power laws; the exponents of these power laws increase markedly with an increase in instability, see Figs. 11–13. It appears that the effect of heating the lower boundary is to increase the scale of the diffusion phenomena without affecting the overall characteristics of the diffusion plume.

Synthetic line source

One can obtain the concentration distribution $C(x, z)$ for a synthetic line source of strength Q_L (mg/cm s) parallel to the y axis and passing through the origin by integrating continuous point sources of strength $Q_f\,dy'$ at y' along this line. If $\chi(x, y, z)$ is the mean concentration at the point (x, y, z) due to turbulent diffusion of mass being emitted from a continuous point source of strength Q_f (mg/s) located at the coordinate orgin, then the synthetic line source concentration is

$$C(x, z) = \int_{-\infty}^{+\infty} \chi(x, y', z)\, dy'. \qquad (7)$$

Now if it is assumed that the transverse profile, for a point source, at each x and z has a Gaussian form, that is,

$$\chi(x, y', z) = \chi(x, 0, z) \exp\left\{-\frac{y'^2}{2p^2}\right\}, \qquad (8)$$

where p is the standard deviation, about the mean, of the assumed Gaussian form, (7) can be integrated to obtain a simple expression for $C(x, z)$. The choice of the Gaussian form is supported by the fact that the exponent "a", for the transverse profiles, in (1) is equal to 2—the expected exponent for a Gaussian form.

Introducing (8) into (7) and evaluating the resulting definite integral one finds that

$$C(x, z) = \sqrt{(2\pi)}\, p(x, z)\, \chi(x, 0, z). \qquad (9)$$

The synthetic concentration distribution shown in Fig. 14 obtained through (9), for both the heated and neutral boundary case, can be represented by the same dimensionless distribution curve as obtained for an actual line source (Poreh [8]),

$$\frac{C(x, z)}{C_{max}(x, 0)} = \exp\left\{-0{\cdot}693\left[\frac{z}{\lambda(x)}\right]^{1{\cdot}8}\right\}, \qquad (10)$$

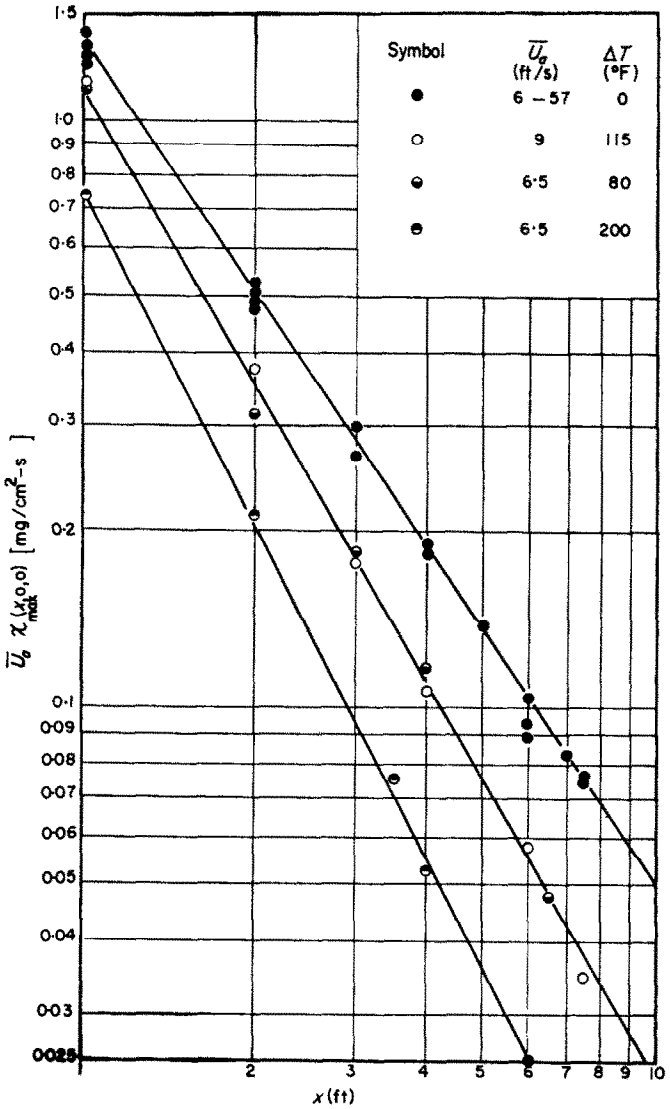

FIG. 11. Effect of instability on the maximum ground-level concentration.

where $\lambda(x)$ is the vertical similarity length of the equivalent line source diffusion plume defined as

$$\frac{C(x, \lambda)}{C_{max}(x, 0)} = 0{\cdot}5.$$

Fig. 15 shows that the heated-boundary data fits equation (10) nicely, whereas there is systematic deviation for the neutral boundary data. This is because the lateral profiles were not mapped completely at the outer edges for the neutral data and thus a larger percentage of mass was neglected in the integration.

The form of the dimensionless distribution appears to be independent of $\bar{U}_a$. The growth of the plume for the neutral case is also independent of $\bar{U}_a$ and is described in Fig. 15. The actual line-source plume (Poreh [8]), behaved in a like manner. The initial variation of $\lambda(x)$ is approximately proportional to $x^{0{\cdot}78}$;

$$\lambda(x) = \text{const. } x^{0{\cdot}78}. \qquad (11)$$

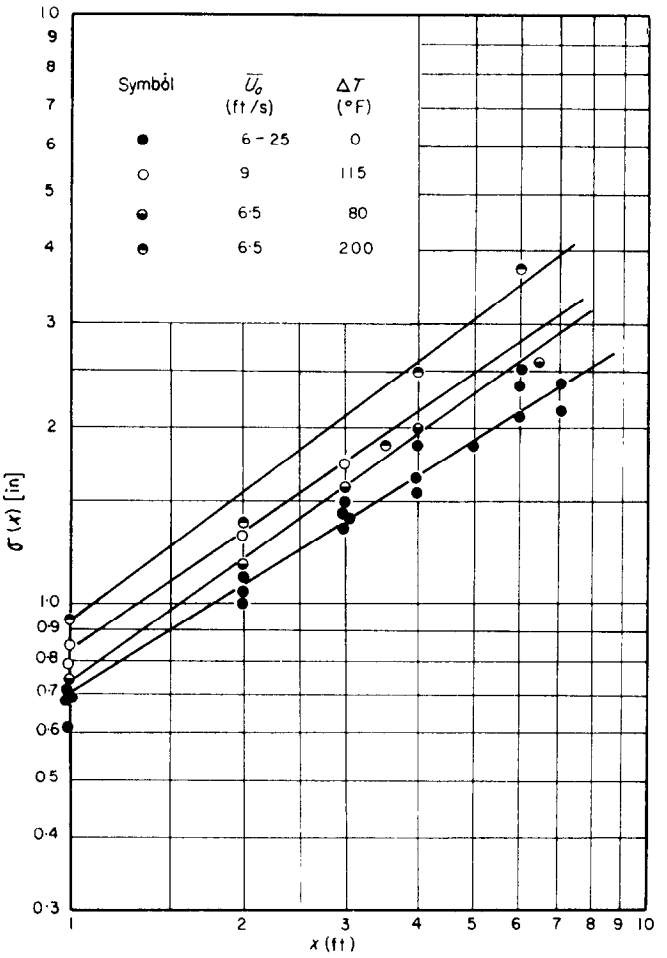

FIG. 12. Effect of instability on the lateral similarity length σ.

Values of $C_{max}(x, 0)$ appear to be inversely proportional to $\bar{U}_a$, as shown in Fig. 15, that is,

$$\bar{U}_a \, C_{max}(x, 0) = \text{const.} \, x^{-0.85}. \quad (12)$$

Poreh [8] also observed this inverse proportionality with $\bar{U}_a$. He obtained $\bar{U}_a \, C_{max}(x, 0) \propto x^{-0.9}$ and $\lambda(x) \propto x^{0.8}$. Thus, the synthetic line-source plume behaves in the same manner as an actual line-source plume for the neutral-boundary case. No actual line-source data were available for comparison with the synthetic heated-boundary data.

Comparison of mass and heat diffusion

Wieghardt [5] obtained data for heat diffusion from a line source of heat located at the bottom of an otherwise isothermal turbulent boundary layer. These data can be compared with the mass diffusion results obtained by Poreh [8] and the synthetic line-source results discussed earlier. The salient results of Wieghardt are the following:

$$\text{(a)} \quad \lambda^*(x) = 1{\cdot}22 \, \lambda_H(x) = \frac{\text{const.} \, x^{0.8}}{(\bar{U}_a/\nu)^{0.2}}, \quad (13)$$

where $\lambda^*(x)$ and $\lambda_H(x)$ are defined as

$$\frac{\bar{i}(x, \lambda^*)}{\bar{i}_{max}(x, 0)} = 0{\cdot}368 \text{ and } \frac{\bar{i}(x, \lambda_H)}{\bar{i}_{max}(x, 0)} = 0{\cdot}5;$$

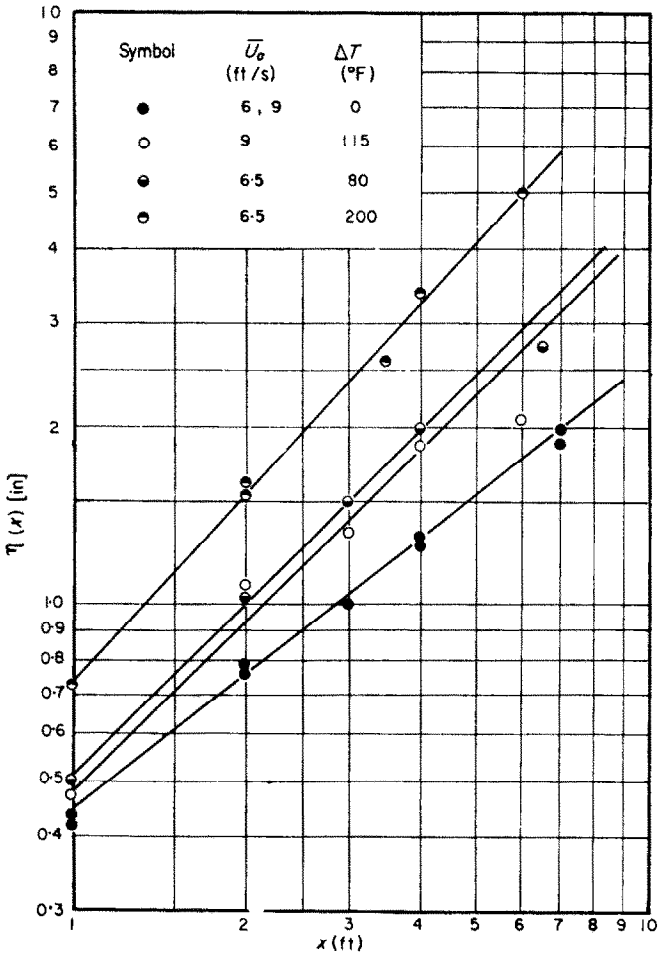

FIG. 13. Effect of instability on the vertical similarity length η.

$$\text{(b)}\quad \frac{\bar{t}(x,z)}{\bar{t}_{\max}(x,0)} = \exp\left\{-\left(\frac{z}{\lambda^*}\right)^{1\cdot8}\right\}; \qquad (14)$$

and

$$\text{(c)}\quad \bar{U}_a\,\bar{t}_{\max}(x,0) = \text{const.}\,\frac{W/B}{\rho\,g\,c_p}\left(\frac{\bar{U}_a}{\nu}\right)^{0\cdot233}\delta^{1/7}\,x^{-0\cdot91}. \qquad (15)$$

It is seen by comparing (10) and (14) that the dimensionless universal distribution function is identical for heat and mass diffusion. Equations (11), (12), (13) and (15) further show that the approximate proportionality of $\lambda_H(x)$ and $\bar{t}_{\max}(x,0)$ with x is also identical with their counterpart in mass-diffusion. The only difference seems to be the slight variation of $\lambda_H(x)$ with $\bar{U}_a^{-0\cdot2}$ and as a consequence $\bar{t}_{\max}(x,0)$ is not quite inversely proportional to $\bar{U}_a$.

The heat diffusion data were for a wide range of ambient velocities (16–93 ft/s) as compared to the range of 9–16 ft/s for the mass diffusion data. Intuitively it would seem that the similarity length $\lambda(x)$ would be a function of $\bar{U}_a$ since at the higher velocities the plume would be swept downstream very rapidly and consequently would be narrower; thus $\lambda(x)$ would be smaller and $\bar{U}_a\,C_{\max}(x,0)$ larger for higher velocities. More mass diffusion data for a wider range of ambient velocities is needed before it can be

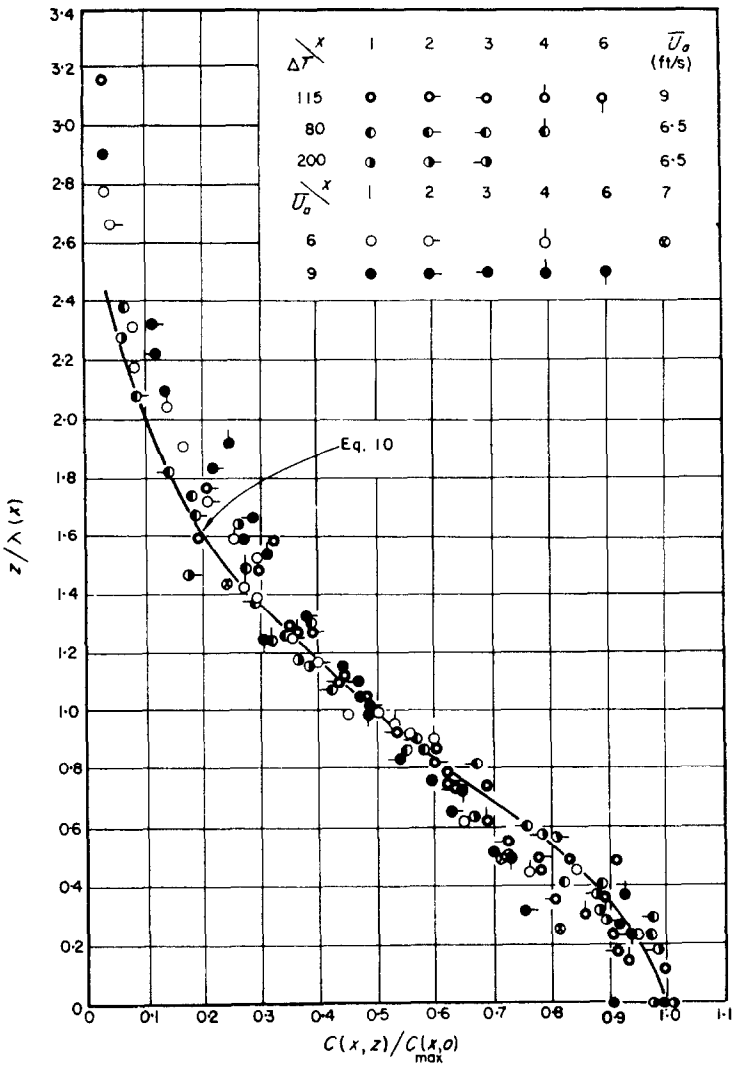

FIG. 14. Relative concentration as a function of the vertical distance for a synthetic line source for heated and unheated boundaries.

established that this apparent difference in heat and mass diffusion exists.

Using the approximate similarity of the scalar and velocity fields one can integrate the diffusion equation

$$\bar{u}\frac{\partial C}{\partial x} + \bar{w}\frac{\partial C}{\partial z} = \frac{\partial}{\partial z}\left[(\gamma + A_z)\frac{\partial C}{\partial z}\right], \qquad (16)$$

or its counterpart for heat diffusion to obtain an expression for A_z or ϵ_H (the diffusivities). Poreh [8] obtained the following expression after performing such an integration, after dropping the molecular diffusion terms;

$$A_z \text{ or } \epsilon_H = -\lambda^{(1+1/n)}\frac{d\lambda}{dx}\delta^{-1/n} f(\bar{U}_a)\frac{S_\lambda(z/\lambda)}{h'(z/\lambda)}\int_0^\infty \left(\frac{z}{\lambda}\right)^{1/n} h\left(\frac{z}{\lambda}\right) d\left(\frac{z}{\lambda}\right), \qquad (17)$$

where $h(z/\lambda)$ is the universal dimensionless

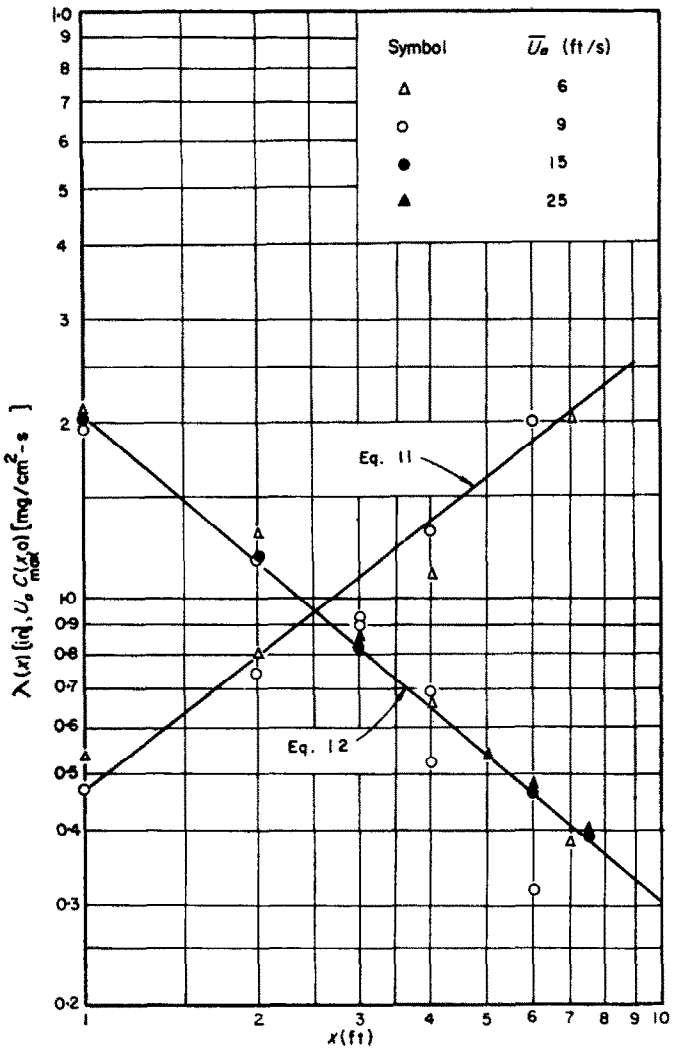

FIG. 15. Variation of the vertical similarity length λ and the maximum ground-level concentration with distance from the synthetic line source for an unheated boundary.

distribution curve and $S_\lambda(z/\lambda)$ is a known function. Using the mean data [Fig. 16 and equations (10–15)] for heat and mass diffusion one obtains $\epsilon_H/A_z = 1{\cdot}8$. This ratio appears unbelievably high. One would expect that the mechanism of heat and mass diffusion are the same (and thus ϵ_H/A_z should be close to 1) since the Prandtl and Schmidt numbers are equal and the differential equations are identical.

This difference may be due to the difference in velocities or the location of the source relative to the beginning of the turbulent boundary layer. In any case more analysis with heat diffusion data obtained in the same wind tunnel and with the sources in the same location is needed before this ratio can be accepted as conclusive.

CONCLUDING REMARKS

The principal results derived from this study

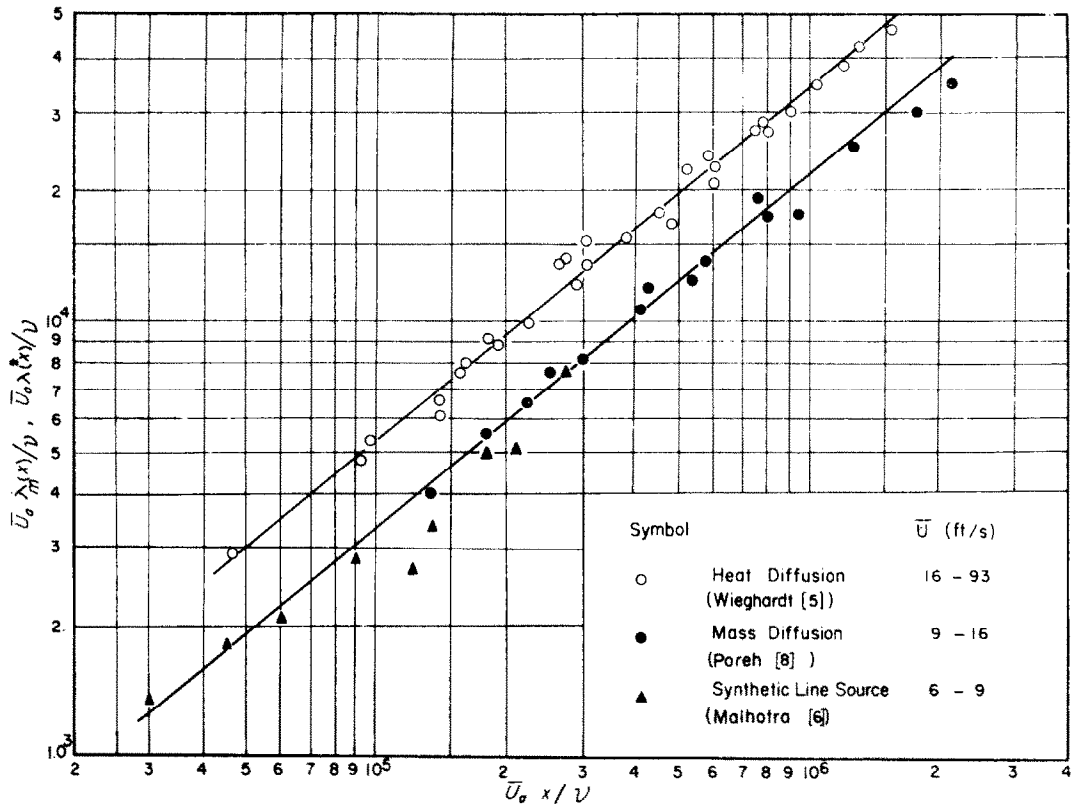

FIG. 16. Comparison of the vertical similarity lengths for line-source diffusion of mass and heat for an unheated boundary.

of turbulent diffusion of mass from a point source *within* a neutral and an unstably stratified boundary layer are:

(a) The concentration distribution, for *both* neutral and unstable conditions, can be described by the same dimensionless distribution function provided diffusion occurs well within the momentum boundary layer.

(b) The lateral and vertical similarity lengths of the diffusion plume are approximately independent of $\bar{U}_a$ for the neutral case. As the degree of instability increases $\sigma(x)$ and $\eta(x)$ increase markedly in magnitude.

(c) The experimental law for attenuation of boundary concentration was obtained as $\chi_{max}(x, 0, 0) \propto x^{-1.5}$ for the neutral case. The rate of attenuation of axial concentration increased with an increase in instability but was not a function of distance downstream from the source in the range studied.

(d) By numerically integrating the point-source plume, assuming that each transverse profile has a Gaussian form, a synthetic line-source plume can be calculated. This synthetic plume compares very favorably with an actual line-source plume, i.e. the concentration distribution can be represented by the same distribution function and the variation of $C_{max}(x, 0)$ and $\lambda(x)$ with distance from the source are the same.

(e) Overall heat and mass diffusion characteristics are very similar for a line source of heat or mass located on the boundary of an isothermal boundary layer-flow. The universal dimensionless distribution curves for mass and heat are the same, and the rate of variation of the similarity lengths and the maximum concentration with distance from the source are the same. The

similarity length and the maximum temperature varied slightly with $\bar{U}_a$ for the heat diffusion case; this dependence on $\bar{U}_a$ could not be detected for the mass-diffusion case.

ACKNOWLEDGEMENTS

The financial assistance received from the National Institutes of Health, U.S. Department of Health, Education and Welfare, for this research is gratefully acknowledged. The assistance of Professor Maxwell Parshall, Department of Civil Engineering, Colorado State University, in the development of the gas sampling and gas analysis systems contributed greatly to this study.

REFERENCES

1. E. M. SPARROW and W. J. MINKOWYCZ, Buoyancy effects on horizontal boundary-layer flow and heat transfer, *Int. J. Heat and Mass Transfer*, **5**, 505–511 (1962).
2. J. E. CERMAK, The turbulent boundary layer at low Reynolds numbers with unstable density stratification. Ph.D. Dissertation, Cornell University, Ithaca, New York (1959).
3. M. L. BARAD, Project Prairie Grass, a field program in diffusion, Vols. I, II. *Geophysics Research Papers*, No. 58, USAF, GRD (1958).
4. D. A. HAUGEN, Project Prairie Grass, a field program in diffusion, Vol. III. *Geophysics Research Papers*, No. 59, USAF, GRD (1959).
5. K. WIEGHARDT, Über Ausbreitungsvorgänge in turbulenten Reibungsschichten, *Z. Angew. Math. Mech.* **28**, No. 11–12, 346–355 (1948).
6. R. C. MALHOTRA, Diffusion from a point source in a turbulent boundary-layer with unstable density stratification. Ph.D. Dissertation, Colorado State University, Fort Collins, Colorado (1962).
7. K. S. DAVAR, Diffusion from a point source within a turbulent boundary-layer. Ph.D. Dissertation, Colorado State University, Fort Collins, Colorado (1961).
8. M. POREH, Diffusion from a line source in a turbulent boundary-layer Ph.D. Dissertation, Colorado State University, Fort Collins, Colorado (1961).

Zusammenfassung—Es wurde turbulente Stoffdiffusion von einer punktförmigen Quelle innerhalb einer zweidimensionalen Grenzschichtströmung an einer glatten Oberfläche mit und ohne Oberflächenheizung untersucht. Die Konzentrationen stromabwärts einer simulierten Punktquelle am Boden einer Windkanalversuchsstrecke wurden mit Ammoniak als diffundierendem Gas ausgemessen.

Die Konzentrationsprofile für neutrale und instabile Bedingungen erweisen sich als ähnlich, d.h. man erhält eine universelle Funktion wenn man $\chi(x, y, z)/\chi_{max}(x, 0, 0)$ die relative Konzentration in jedem Abschnitt als Funktion der Ähnlichkeitslängen $\sigma(x)$ und $\eta(x)$ auffasst. Die Ähnlichkeitslängen sind als $\chi(x, \sigma, 0)/\chi_{max}(x, 0, 0) = 0{,}5$ und $\chi(x, 0, \eta)/\chi_{max}(x, 0, 0) = 0{,}5$ definiert; es zeigt sich, dass sie im Bereich 1,8–7,5 m/s annähernd unabhängig von der Umgebungsgeschwindigkeit sind und mit zunehmender Instabilität eine ausgeprägte Vergrösserung zeigen.

Eine Methode zur numerischen Integration der Werte punktförmiger Quellen, um federförmige Linienquellen zu erhalten, ist angegeben. Die so erhaltenen künstlichen federförmigen Linienquellen werden mit tätsächlichen Werten von Linienquellen und mit Werten linienförmiger Wärmediffusionquellen verglichen. Die Werte der Wärme- und Stoffdiffusion sind sehr ähnlich.

Ein Versuch wurde unternommen, das Verhältnis der Wärmediffusion zur Stoffdiffusion durch Integration der zweidimensionalen Diffusionsgleichung zu erhalten mit Hilfe der angenäherten Ähnlichkeit der Konzentrations- und Geschwindigkeitsverteilungen. Für das Verhältnis ergab sich der ungefähre Wert 1,8.

Аннотация—Исследовалась турбулентная диффузия вещества от точечного источника в плоском пограничном слое у гладкой поверхности при нагреве стенки и без него. В качестве диффундирующего газа использовался аммиак. Измерялось изменение его концентрации вниз по течению от точечного источника, расположенного в нижней стенке рабочей части аэродинамической трубы.

Установлено подобие профилей концентрации для нейтральных и неустойчивых условий. Таким образом, относительную концентрацию $\chi(x, y, z)/\chi_{max}(x, 0, 0)$ в каждом сечении можно представить как функцию масштабовп одобия $\sigma(x)$ и $\eta(x)$, т.е. можно получить универсальную функцию. Масштабы подобия определяются как

$$\chi(x, \sigma, 0)/\chi_{max}(x, 0, 0) = 0{,}5 \quad \text{и} \quad \chi(x, 0, \eta)/\chi_{max}(x, 0, 0) = 0{,}5$$

и в первом приближении не зависят от скорости набегающего потока в интервале 6–25 фт/сек, заметно возрастая с ростом неустойчивости.

Рассматривается метод численного интегрирования для получения струек линейного источника. Искусственные струйки линейного источника, полученные таким

образом, сравниваются с фактическими данными диффузии тепла и вещества от линейного источника. Данные по диффузии тепла и вещества весьма сходны.

Сделана попытка определить соотношение между коэффициентами диффузии тепла и массы вещества путём интегрирования уравнения двухмерной диффузии с использованием приближённого подобия распределения концентрации и скорости. Найдено, что величина этого соотношения составляет примерно 1,8.